International Journal of Electrical and Power Engineering 1 (2): 138-145, 2007

Parametric Analysis by the Meshless Local Petrov Galerkin (MLPG) Approach Applied to Electromagnetic Problems

N. Benbouza, F.Z. Louai, S. Drid and A. Benoudjit
Laboratory of Electromagnetic Systems-Propulsion Induction LSP-IE Batna,
Department of Electrical Engineering, Faculty of Engineering, University of Batna,
Street Chahid Med El Hadj Boukhlouf, 05000-Batna, Algeria

Abstract: Meshless or element free methods are a new class of numerical techniques as alternatives to the popular Finite Element Method (FEM) for solving partial differential equations. The solution is entirely built in terms of a set of distributed nodes, thus no element connectivity is required. The meshless local Petrov-Galerkin method based on the moving least squares approximation is one of the recent meshless approaches. By a judicious choice of the test and trial functions, a weighted residual form is applied to a local sub-domain and makes the method truly meshless. In this study, the method is presented to study electromagnetic field problems both in one-Dimensional (1D) and two-Dimensional (2D). The formulations were implemented using a penalty approach to enforce essential boundary conditions. The sensitivity of several parameters of the method was mainly studied and discussed by comparing results with those calculated using the difference finite method. Very accurate solutions could be obtained by a judicious choice of these parameters.

Key words: Moving Least Square (MLS) approximation, local week form, weight and test functions, domain of influence, gauss integration, penalty approach, Meshless Local Petrov Galerkin (MLPG) method

INTRODUCTION

To eliminate the burdensome mesh generations of traditional numerical methods such as the finite element approach, increasing attention and efforts have been paid to meshless methods. Basically, these methods consist of the discretisation of the problem domain and its boundary by a set of scattered points. The shape function for each point is then built using its influence domain, which defines the relationship between the point and its neighbors (Guangzheng *et al*., 2003; Viana *et al*., 2004).

Some of the most widely used meshless methods are the Smooth Particle Hydrodynamics (SPH), Diffuse Element Method (DEM), Element Free Galerkin method (EFG), hp-clouds method Finite Point Method (FPM) and so on. However, some of these methods are not really meshless methods, since they employ a background grid for the numerical integration process in the solution domain (Viana *et al*., 2004; Lin *et al*., 2000). A truly meshless method called the Mesheless Local Petrov Galerkin (MLPG) method Atluri and Zhu (1998) has attracted a lot of attention and extended too many problems. It does not require a mesh either for the approximation of the trial function or for the integration of the week form. This approach uses Petrov Galerkin method instead of the traditional Galerkin procedure to develop the discrete equations. The method is based on a weak form computed over a local defined shape sub-domain and derived by using the test and trial functions from different functional spaces (Guangzheng *et al*., 2003; Viana *et al*., 2004; Lin *et al*., 2000; Atluri and Zhu, 1998; Raju and Chen, 2001, 2003; Philips, 2002). The shape functions are constructed by the moving least squares interpolations.

In the present research, an MLPG algorithm is implemented for electromagnetic field problems and aims the sensibility and effectiveness of the method to various parameters using two numerical applications. To this end, the numerical method is presented briefly. Next, the moving least squares interpolation is described. Than, the discretisation procedure and the discrete formulations together with the penalty approach are presented. Various choices of the parameters are studied by evaluating and examinating the accuracy. Finally, conclusions are drawn.

Corresponding Author: N. Benbouza, Laboratory of Electromagnetic Systems-Propulsion Induction LSP-IE Batna, Department of Electrical Engineering, Faculty of Engineering, University of Batna, Street Chahid Med El Hadj Boukhlouf, 05000-Batna, Algeria

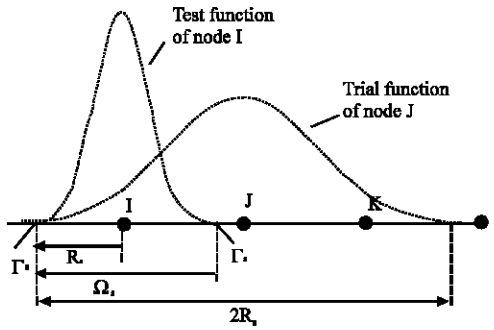

Fig. 1: Comparison of the trial and test function domains (1D case)

PRINCIPLE OF THE MLPG METHOD

In the traditional element free Galerkin method, the test and trial function are chosen from the same space. The domain of integration for the I-J term in the weak form is the intersection of these functions and its shape is difficult to determine in 2D or 3D. The need of using a shadow mesh negates the advantages of the method. To develop a truly meshless method, Alturi and Zhu suggested the choice of the test function functions from different spaces and make this a Petrov Galerkin method. The test functions are chosen such that they are non-zero over an arbitrary shape of sub-domain $\bullet_s$ similar to the weight functions. Hence, the test functions have well defined geometric shapes such as a circle, a square, a rectangle or an ellipse (in 2D). Thus, the integrations over the entire domain $\bullet$ can be restricted to $\bullet_s$ limited by $\bullet_s$, this choice eliminates the need of shadow (Fig. 1) mesh and the method is truly meshless (Atluri and Zhu, 1998; Raju and Chen, 2001, 2003; Philips, 2002).

THE MLS APPROXIMATION
(Lin, 2000; Atluril, 2000; Raju, 2001; 2003; Philips, 2002; Dolbow, 1998)

The MLPG method employs Moving Least Squares (MLS) approximation witch is generally considered as one of the schemes to interpolate data with a reasonable accuracy.

The approximation $u^h(X)$ of the unknown function u(X) is defined by:

$$u^h(X) = \sum_{j=1}^{m} p_j(X)a_j(X) = p^T(X)a(X) \quad (1)$$

Where $a_j(X)$ are unknown parameters varying with X such as:

$$X = [\,x\,] \text{ in 1D} \quad (2)$$
$$X^T = [x, y] \text{ in 2D}$$

$$a^T(X) = [a_0(X) \quad a_1(X) \quad a_2(X) \quad \ldots \quad a_m(X)] \quad (3)$$

and P(X) is the basis of a complete polynomial of order m Linear basis:

$$P^T(m = 2) = \{\,1, x\,\} \text{ in 1D}$$
$$P^T(m = 3) = \{\,1, x, y\} \text{ in 2D} \quad (4)$$

Quadratic basis:

$$P^T(m = 2) = \{1, x, x^2\} \text{ in 1D}$$
$$P^T(m = 3) = \{\,1, x, y, x^2, xy, y^2\} \text{ in 2D} \quad (5)$$

Consider a sub-domain $\bullet_x$ the neighborhood of a point X; the local approximation at point X is given by

$$u_L^h(X_I, X) = \sum_{j=1}^{m} p_j(X_I)a_j(X) = p^T(X_I)a(X) \quad (6)$$

The unknown coefficientsat $a_j(X)$ any point in $\bullet_x$ are determined by minimizing the quadratic functional:

$$J(X) = \sum_{I=1}^{n} \omega(X - X_I)\left[u_L^h(X_I, X) - u_I\right]^2$$
$$= \sum_{I=1}^{n} \omega_I(X)\left[P^T(x_I).a(X) - u_I\right]^2 \quad (7)$$

where $\bullet_I(X) = \bullet\,(X\text{-}X_I)$ is a weight function associated with the node I and n is the number of nodes in the small domain $\bullet_x$ for witch $\bullet_I(X) \bullet 0$.
u_I are the fictitious nodal values of u at $X=X_I$. With:

$$u^T = [\,u_1, u_2, \ldots\ldots\ldots, u_n\,] \quad (8)$$

The stationarity of J with respect to a(X) leads to the following linear relation between a(X) and u_I.

$$a(X) = A^{-1}(X).B(X).u \quad (9)$$

where: $$A(X) = \sum_{I=1}^{n} \omega_I(X)\, p(X_I)\, p^T(X_I) \quad (10)$$

$$B(X) = [\omega(X\text{-}X_1).P(X_1) \ldots \omega(X\text{-}X_n)P(X_n)] \quad (11)$$

Very similar to that in FEM, the MLS approximation $u^h(X)$ is written as:

$$u^h(X) = \sum_{I=1}^{n} \varphi_I(X)\, u_I = \varphi(X) u^T \quad (12)$$

where $\varphi_I(X)$ is the shape function of node I and is defined as:

$$\varphi_I(X) = P^T(X).A^{-1}(X).B_I(X) \quad (13)$$

The shape function does not pass through the fictitious nodal values used to fit them, thus they do not satisfy the Kronecker delta criterion: $\varphi_I(X_J) = \delta_{IJ}$ so $u^h(X_I) \neq u_I$. Therefore, imposition of essential boundary conditions is difficult. In our implementation, the penalty approach is used to enforce these conditions.

In (8) and (9) equation $\omega_I(X)$ is a compactly supported weight function centered at node I, the support of a node I is called often the domain of influence. In this study, the cubic spline, quartic spline and exponential weight functions were used:

Quartic spline:

$$\omega(r) = \begin{cases} 1-6r^2+8r^3-3r^4 & \text{if } r \leq 1 \\ 0 & \text{if } r > 1 \end{cases} \quad (14)$$

Cubic spline:

$$\omega(r) = \begin{cases} 2/3 - 4r^2 + 4r^3 & \text{si } r \leq 1/2 \\ 4/3 - 4r + 4r^2 - 4/3\, r^3 & \text{si } 1/2 < r \leq 1 \\ 0 & \text{si } r > 1 \end{cases} \quad (15)$$

Exponential:

$$\omega(r) = \begin{cases} e^{-(r/0.4)^2} & \text{si } r \leq 0 \\ 0 & \text{si } r > 0 \end{cases} \quad (16)$$

where r is the normalized distance given by:

$$r = d_I / R_I \quad (18)$$

d_I : is the distance between the center of sub-domain of influence X_I and general point X, so:

$$d_I = \left| X - X_I \right| \quad (19)$$

R_I: is the domain of influence size at node I and it is computed by:

$$R_I = dmax_I . c_I \quad (20)$$

where $dmax_I$ is a scaling parameter and C_I is the difference between node X_I and its neighbor, it is chosen such that matrix A is non singular. If the nodes are uniformly spaced, the value of correspond to the step h of the nodal distribution ($C_I = h$).

In 2D, the domain of influence node's covers an area and its corresponding weight function is derived as a tensor product weight which can be expressed as:

$$\omega_I(X) = \omega(r_x)\, \omega(r_y) \quad (21)$$

where $\omega(r_x)$ and $\omega(r_y)$ are given by Eq. 14-16 with *r* replaced by or given by:

$$r_x = \left| x - x_I \right| / R_{xI} ; r_y = \left| y - y_I \right| / R_{yI} \quad (22)$$

The choice of c_{xI} and c_{yI} is similar to the process used below. In this research, a square domain is chosen as domain of influence of a node.

INTEGRAL FORMULATIONS

1D case: Consider the following 1D Poisson problem in the domain

$$\Omega : d^2u/dx^2 = p \quad (23)$$

The essential and natural boundary conditions are, respectively:

$$u = u_0 \text{ on } \Gamma_u \text{ and } q = q_0 \text{ on } \Gamma_q \quad (24)$$

Where: $\Gamma_u \cup \Gamma_q = \Gamma$ is the boundary of Ω and $q = du/dx$ is the normal flux.

In a sub-region Ω_s, which is located entirely inside the global domain, the local weighted residual form is used to implement the MLPG formulation. The essential boundary conditions are included by the penalty method as (Philips, 2002):

$$\int_{\Omega s} \left(\frac{d^2u}{dx^2} + p\right).v.dx + \alpha \int_{\Gamma su} (u - u_o).v d\Gamma \quad (25)$$

where u is the trial function obtained using MLS approximation, is the test function, α is the penalty parameter chosen as a large number ($\alpha >> 1$) and Γ_{su} is a part of the boundary Γ_u of Ω_s over which the boundary conditions are specified such as : $\Gamma_{su} = \Gamma_s \cap \Omega$.

As in one dimensional problems, the boundaries are points; the second integral in (25) is evaluated with the Dirac delta function:

$$\int_{\Gamma su} (u - u_o).v\ \delta(X = X_{\Gamma su})d\Gamma = \left[\alpha(u - u_o)v\right]_{\Gamma su} \quad (26)$$

By replacing (26) into (25) and integrating by part, the local weak form can be written as:

$$\int_{\Omega_s} \frac{du}{dx}\frac{dv}{dx}dx + \int_{\Omega_s} pvdx + \alpha\left[(u - u_0)v\right]_{\Gamma_{su}} + -\left[vq\right]_{\Gamma_s} = 0 \quad (27)$$

where $\bullet_s$ is broken into subsets:
$\bullet_{sq} = \bullet_s \bullet_q$, $\bullet_{su} = \bullet_s \bullet_u$ and $\bullet_s$

$\bullet_s$ completely within interior of $\bullet$ (Philips, 2002). Then:

$$\int_{\Omega s} \frac{du}{dx}\frac{dv}{dx}dx + \int_{\Omega s} p.v.dx + \alpha\left[(u - u_o)v\right]_{\Gamma su} + -\left[v.q\right]_{\Gamma su} - \left[v.q_o\right]_{\Gamma sq} = 0 \quad (28)$$

As mentioned previously, the test functions can be chosen to vanish on $\bullet_s$, the term $[vq]\bullet_s$ is therefore evaluated as zero. Then the weak form, leads to the resulting system of equations:

$$k^{node}\ u + k^{bdry}\ u = f^{node} + f^{bdry} \quad (29)$$

where node and bdry denotes internal and boundary nodes, respectively.

$$k_{ij}^{(node)} = \int_{\Omega_s} \frac{dv_i}{dx}\frac{d\phi_j}{dx}dx \quad (30)$$

$$k_{ij}^{(bdry)} = [\alpha\ v_i\ \phi_j]_{\Gamma_{su}^{(i)}} - [v_i \frac{d\phi_j}{dx}]_{\Gamma_{su}^{(i)}} \quad (31)$$

$$f_i^{(node)} = -\int_{\Omega_s^{(i)}} pv_i\,dx \quad (32)$$

$$f_i^{(bdry)} = [\alpha\ u_o\ v_i]_{\Gamma_{su}^{(i)}} + [vq_o]_{\Gamma_{sq}^{(i)}} \quad (33)$$

The conventional Gaussian integration is used as a numerical integration to evaluate the integrals involved in Eq. 30 and 32. The order of integration required for acceptable results depends on the basis and weight functions used.

2D case: For illustrative purposes, let us consider the following 2D Poisson problem, in domain $\bullet$ enclosed by $\bullet$:

$$\frac{\partial^2 u}{\partial x^2} + \frac{\partial^2 u}{\partial y^2} = p \quad (34)$$

$$u = u_0 \text{ on } \Gamma_u \text{ and } q = q_o \text{ on } \Gamma_q \quad (35)$$

where $q = du/dn$ and n is the outward normal direction to $\bullet$.

So, using the divergence theorem, the local weak form of governing equation will be (Atluri and Zhu, 1998):

$$\int_{\Omega_S} (\frac{\partial u}{\partial x}\frac{\partial v}{\partial x} + \frac{\partial u}{\partial y}\frac{\partial v}{\partial y})d\Omega + \alpha\int_{\Omega_S} uvd\Omega - \int_{\Gamma_{su}} qvd\Gamma = \int_{\Gamma_{su}} q_0 vd\Gamma + \alpha\int_{\Gamma_{su}} u_0 vd\Gamma - \int_{\Omega_S} Pvd\Omega \quad (36)$$

Substitution of the trial and test functions, in the weak form, leads to the resulting element matrix:

$$k_{ij}^{(node)} = \int_{\Omega_s^{(i)}} (\frac{\partial \phi_j}{\partial x}\frac{\partial v_i}{\partial x} + \frac{\partial \phi_j}{\partial y}\frac{\partial v_i}{\partial y})d\Omega \quad (37)$$

$$k_{ij}^{(bdry)} = \alpha\int_{\Gamma_{su}^{(i)}} \phi_j v_i d\Gamma - \int_{\Gamma_{su}^{(i)}} \frac{\partial \phi}{\partial n} v_i d\Gamma \quad (38)$$

$$f_i^{(node)} = \int_{\Omega_s^{(i)}} pv_i d\Omega \quad (39)$$

$$f_i^{(bdry)} = \alpha\int_{\Gamma_{su}^{(i)}} u_0 v_i d\Gamma - \int_{\Gamma_{sq}^{(i)}} q_0 v_i d\Gamma \quad (40)$$

As in 1D, numerical integration of Gauss is used to evaluate the integrals involved in Eq. 37-40 in every sub-domain.

Choice of the test function: In the present research, the test function is defined in a similar manner as the weight function in the MLS approximation, by replacing the R_i with Ro. For the quartic spline case:

$$v(r) = \begin{cases} 1\text{-}6r^2 + 8r^3\text{-}3r^4 & \text{if } r \le 1 \\ 0 & \text{if } r \succ 1 \end{cases} \quad (41)$$

where r is the normalized distance given by:

$$r = \left|X\text{-}X_I\right| / R_o \quad (42)$$

R_o is a user defined parameter that determines the extent of the test function and hence • s. It is computed by using another scaling factor $dmax_2$ by the relation:

$$R_o = dmax_2 c_I \quad (43)$$

In the previous equations, the basis sub-region Ω_s^I is the support domain of v1 (X)of node I. As for the weight function, it is assumed to be a square of side 2Ro, centered at the point in question and it has sides parallel to the coordinate's axis.

RESULTS AND DISCUSSION

One dimensional application model: The proposed method was applied to a 1D electrostatic model with tree different middles and two essentials conditions: u_0=1V and u_L =10V (Fig. 2). The uniform relative permittivity and the constant electric charge density for every region are shown in the Table 1. The first calculation uses the linear basis function and the quartic spline as weight function.

The scaling factors are set to $dmax_1$ = 2 and $dmax_2$ = 3. These values were used at all nodes, except at nodes (2, N-1 and 3 , N-2). For the first couple: $dmax_2$ = 1 and for the second $dmax_2$=2 were used to ensure a symmetric • $_s$, the test function were chosen to vanish on such as • $_i$ =0 on for node i (Philips, 2002). The results are computed at N = 31 uniformly spaced nodes using PG = 8 Gaussian quadrature points in each local domainwith a penalty coefficient • = 10^5. The computed solution of the electric scalar potential u was compared to the finite difference one

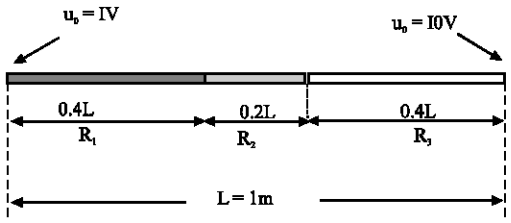

Fig. 2: 1D Electrostatic model

Table 1: Regions characteristics

	R_1	R_2	R_3
•$_r$	1	10^{10}	10^5
• (c/m)	0	1.3	0

Table 2: Regions characteristics

	R_1	R_2	R_3	R_4
μ_r	10	10^5	10^5	1
jex (A/m^2)	0	3.10^5	-3.10^5	0

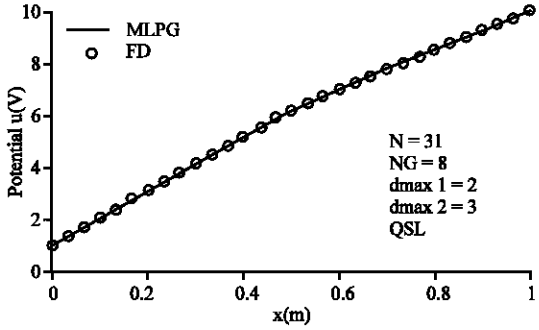

Fig. 3: MLPG and DF scalar potential

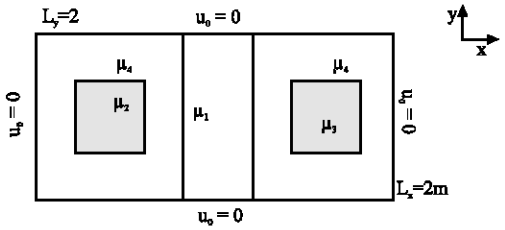

Fig. 4: 2D magnetic model

and represented in Fig. 3. As would be expected, a good agreement between the two solutions is noticed.

Two dimensional application model: The MLPG method is applied to a two dimensional magnetic problem of Poisson equation showed in Fig. 4 and which characteristics are given in Table 2. The solution is calculated using a linear basis function and the precision is evaluated using the FD method.

Uniform mesh of 24×24 nodes is used. The scaling factors are taken to be $dmax_1$ = 1.2 and $dmax_2$ = 2 for every node. In this example, 3 Gauss points are used on each section of and 6×6 points in the local domain with • = 10^5. Potential distributions, equipotential contours for MLPG and DF solutions are shown in Fig. 5-7. In this case also, good similitude is noted between results.

Problem parameters: In the applications of the MLPG method, several parameters are user-controlled, so to evaluate their effects on MLPG solution, the following error norm is used:

$$|e| = \sqrt{\frac{1}{N}\sum_{I=1}^{n}\left(\left(\frac{u_{MLPG} - u_{exact}}{u_{exact}}\right)_i\right)^2} \quad (44)$$

where N is the total number of distributed internal points in the studied domain, the norm is calculated in decimal logarithm for the cubic, quartic and exponential weight functions both in a linear (CSL, QSL, EL) and a

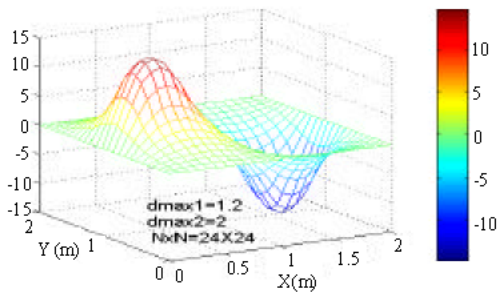

Fig. 5: MLPG potential magnetic vector

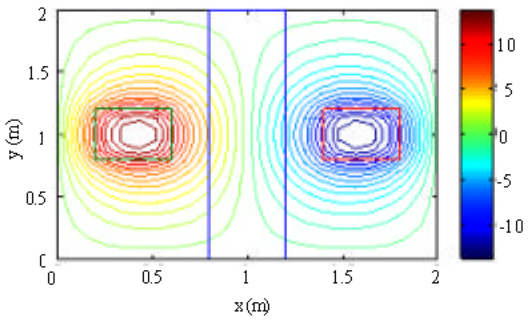

Fig. 6: MLPG equipotential contours

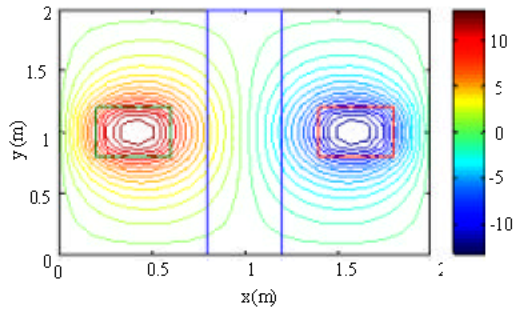

Fig. 7: DF equipotential contours

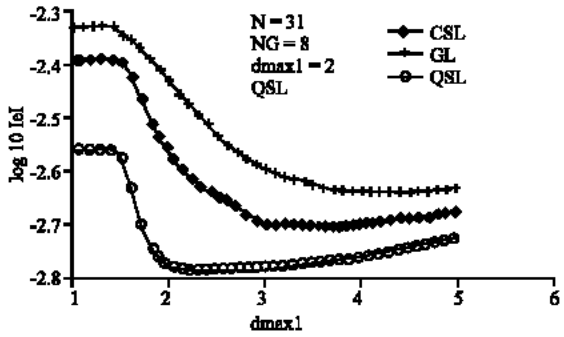

Fig. 8: Variation of error norm with $dmax_1$

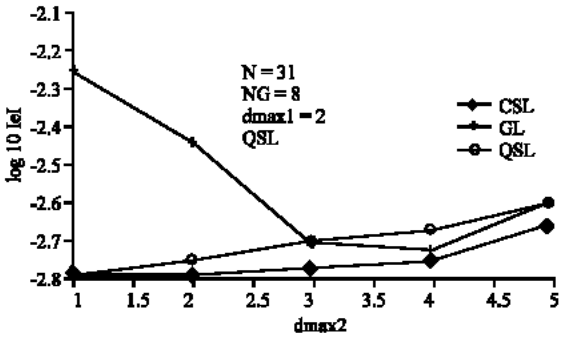

Fig. 9: Variation of error norm with $dmax_2$

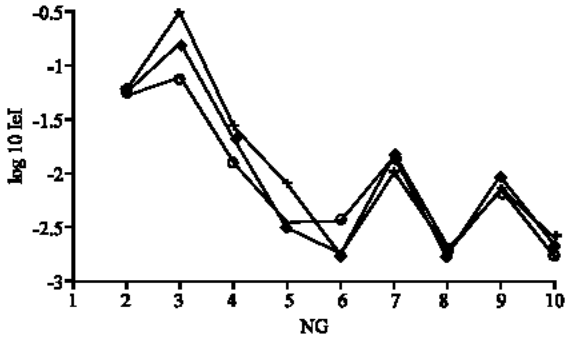

Fig. 10 Variation of error norm with NG

quadratic (CSQ, QSQ, EQ) basis functions. The calculations were carried out using the 1D previous model. The effect of the scaling parameters was evaluated by varying them in the range (Guangzheng *et al*., 2003; Viana *et al*., 2004; Lin *et al*., 2000; Atluri and Zhu, 1998; Raju and Chen, 2001) using the previous values of N, PG and •. A good accuracy is reached for QSL function in the range (Viana *et al*., 2004; Lin *et al*., 2000) for $dmax_1$ (Fig. 8) and in the range (Guangzheng *et al*., 2003; Viana *et al*., 2004) for $dmax_2$ for EL and QSL (Fig. 9). Then Gauss point's number is varied from 1 to 10 using the same values of the other factors. In Fig. 10, error curves show a minimum at PG = 8 for the CSL. Note that for PG = 1 the resulting matrix is singular. Finally, the effect of the nodal arrangement on the error norm is shown in Fig. 11. All models yields accurate solutions, so increasing the number of nodes in the model increases the accuracy of the result, thus the size of • $_s$ also decreases.

In this second part, the error is calculated for a quadratic basis according to the same previous steps. For the first calculation, results show that for the values of $dmax_1<2$, certain matrices are singular, calculation is then made for $dmax_1>2.01$. In Fig.12, high values of error norm are noticed at 2.01. Curves show that errors generated by the functions CSQ and EQ presents almost the same values in the neighborhood of -2.8. Thus the value $dmax_1 = 3$ is used for the remainder of calculation. For the

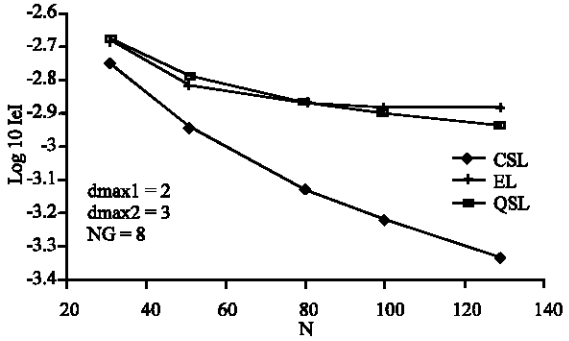

Fig. 11 Variation of error norm with N

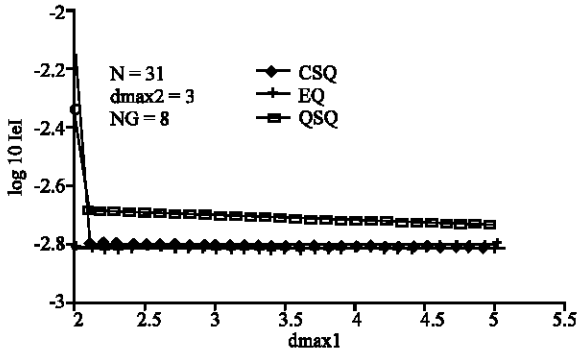

Fig. 12 Variation of error norm with $dmax_1$

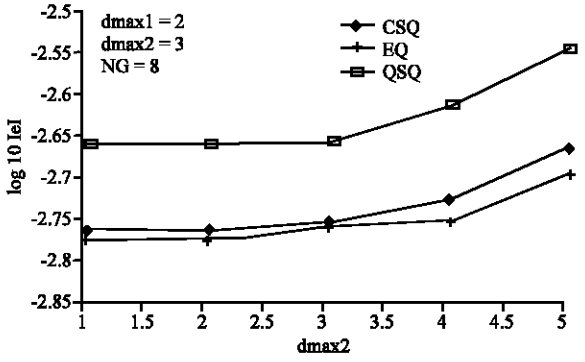

Fig. 13 Variation of error norm with $dmax_2$

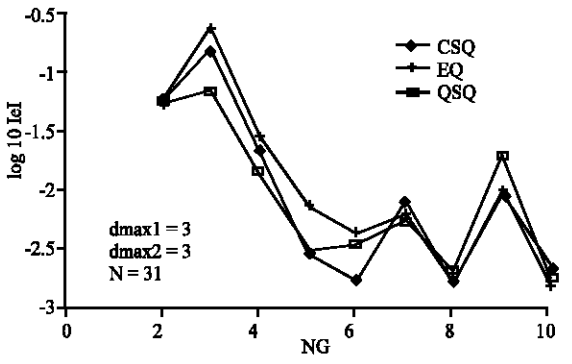

Fig. 14 Variation of error norm with NG

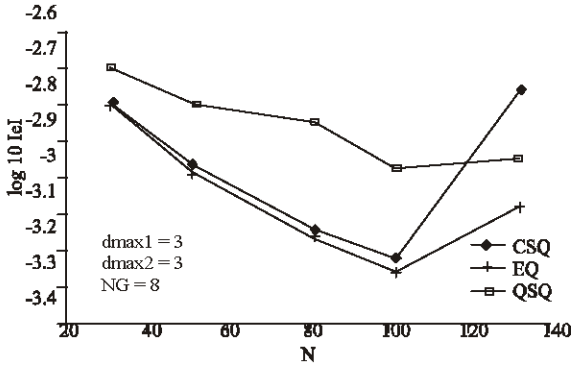

Fig. 15 Variation of error norm with N

variation of $dmax_2$, weak values of errors are reached at 1 and 2 values after what, the error increases for the three functions (Fig. 13).

The effect of NG number is then given by Fig. 14, the EQ curve error shows a minimum at NG = 8. The influence of the step mesh on the solution is also studied. Figure 15 shows that when the step decreases the error decreases but increases after N = 101 nodes. In this case, the values of $dmax_1$, $dmax_2$ and NG can not obligatorily generate a good precision for all models.

CONCLUSION

The MLPG method is a very recent numerical one and is very attractive for the resolution of the partial differential equations because it does not need the mesh imposed by the finite element method.

This present reserch proposes the application of the MLPG method to simulation of electromagnetic problems with inhomogeneous domain of analysis. The aim had is to study the influence of various factors appearing in the discrete equations of the problem. The study was made on a set of equidistant nodes and the following conclusions could be drawn:

- The linear basis avoids the singularity of the matrices.
- A good accuracy could be obtained for larger domain of influence of weight functions and lowest size support domain of test functions.
- With the increase of the domain influence, the cost of memory for saving global stiffness matrix and computational time would be increased.
- Increase the number of nodes does not imply a reduction in the error and depends on the choice of the parameter dmax.
- A large number of Gauss points is necessary for an accurate solution.

- For the quadratic basis, the exponential gives more accurate results. For a linear basis, the cubic spline function is preferred.

One noticed the very weak order of the error norm found in each stage of calculation. The results obtained by the MLPG method conform very well with the DF results by making a suitable choice of the various parameters used.

REFERENCES

Atluri, S.N. and T. Zhu, 1998. A new meshless local Petrov-Galerkin (MLPG) approach in computational mechanics. Los Angeles CA 900995-1600, USA.

Dolbow, J. and T. Belytshko, 1998. An Introduction to Programming the Meshless Element Free Galerkin Method, Arch. Computational Met. Eng., 05: 207-241.

Guangzheng, N.I., Yongjie Zhang, N.I. Peihong, Shiyou Yangl, 2003. Meshless Local Petrov-Galerkin Method and its Application to Electromagnetic Field Computations, 11th International Symposium on Electromagnetics and Mechanics (ISEM).

Lin, H., S.N. Atluri1 and Ni, 2000. Meshless Local Petrov-Galerkin (MLPG) Method for Convection-Diffusion Problems, CMES., 2: 45-60.

Philips, D.R., 2002. Meshless Local Petrov-Galerkin Method for Bending Problems. Langley Research Center, Hampton, Virginia NASA/TM-2002-211936.

Raju, I.S. and T. Chen, 2001. Meshless Petrov-Galerkin method applied to axisymmetric problems. Chen NASA Langley Research Center, Hampton, VA 23681-0001, U.S.A. AIAA-1253.

Raju, I.S. and T. Chen, 2003. A computationally efficient meshless local Petrov-Galerkin method for axisymmetric problems. NASA Langley Research Center Hampton, VA 23681, AIAA-1673.

Viana, S.A., D. Rodger and H.C. Lai, 2004. Meshless local Petrov-Galerkin method with radial basis functions applied to electromagnetics, IEEE. Proc. Sci Meas. Tech., pp: 151- 6.